

# **Reduced order modeling and analysis of the human complement system**

Adithya Sagar, Wei Dai<sup>#</sup>, Mason Minot<sup>#</sup>, and Jeffrey D. Varner\*

School of Chemical and Biomolecular Engineering

Cornell University, Ithaca NY 14853

**Running Title:** A reduced order model of complement

**To be submitted:** *Scientific Reports*

# Denotes equal contribution

\*Corresponding author:

Jeffrey D. Varner,

Professor, School of Chemical and Biomolecular Engineering,

244 Olin Hall, Cornell University, Ithaca NY, 14853

Email: jdv27@cornell.edu

Phone: (607) 255 - 4258

Fax: (607) 255 - 9166

## Abstract

Complement is an important pathway in innate immunity, inflammation, and many disease processes. However, despite its importance, there have been few validated mathematical models of complement activation. In this study, we developed an ensemble of experimentally validated reduced order complement models. We combined ordinary differential equations with logical rules to produce a compact yet predictive complement model. The model, which described the lectin and alternative pathways, was an order of magnitude smaller than comparable models in the literature. We estimated an ensemble of model parameters from *in vitro* dynamic measurements of the C3a and C5a complement proteins. Subsequently, we validated the model on unseen C3a and C5a measurements not used for model training. Despite its small size, the model was surprisingly predictive. Global sensitivity and robustness analysis suggested complement was robust to any single therapeutic intervention. Only dual dual-knockdown of both C3 and C5 consistently reduced C5a formation when all pathways were activated. Taken together, we developed a reduced order complement model that was computationally inexpensive, and could easily be incorporated into pre-existing or new pharmacokinetic models of immune system function. The model described experimental data, and predicted the need for multiple points of therapeutic intervention to disrupt complement activation.

**Keywords:** Complement system, systems biology, reduced order models, biochemical engineering

## **1 Introduction**

2 Complement is an important pathway in innate immunity. It plays a significant role in  
3 inflammation, host defense as well as many disease processes. Complement was dis-  
4 covered in the late 1880s where it was found to 'complement' the bactericidal activity of  
5 natural antibodies (1). However, research over the past decade has shown that the im-  
6 portance of complement extends well beyond innate immunity. For example, complement  
7 contributes to tissue homeostasis by inducing tissue repair (2). Complement has also  
8 been linked with several diseases including Alzheimers, Parkinson's disease, multiple  
9 sclerosis, schizophrenia, rheumatoid arthritis and sepsis (3, 4). Complement plays both  
10 positive and negative roles in cancer; attacking tumor cells with altered surface proteins  
11 in some cases, while potentially contributing to tumor growth in others (5, 6). Lastly, sev-  
12 eral other important biochemical subsystems are integrated with complement including  
13 the coagulation cascade, the autonomous nervous system and inflammation (6). Thus,  
14 complement is important in a variety of beneficial and potentially harmful functions in the  
15 body.

16 The complement cascade involves over 30 soluble and cell surface proteins, receptors  
17 and regulators. The molecular connectivity of complement is complex, see the review of  
18 Walport (7, 8). The central outputs of complement are the Membrane Attack Complex  
19 (MAC), and the inflammatory mediator proteins C3a and C5a. The membrane attack  
20 complex, generated during the terminal phase of the response, forms transmembrane  
21 channels which disrupt the membrane integrity of targeted cells, leading to cell lysis and  
22 death. On the other hand, the C3a and C5a proteins act as a bridge between innate and  
23 adaptive immunity, and play an important role in regulating inflammation (5). Complement  
24 activation takes places through three pathways: the classical, the lectin binding and the  
25 alternate pathways. Each of these pathways involves a different initiator signal which trig-  
26 gers downstream events in the complement system. The classical pathway is triggered

27 by antibody recognition of foreign antigens or other pathogens. A multimeric protein com-  
28 plex C1 binds to antibody-antigen complexes and undergoes a conformational change,  
29 leading to an activated form with proteolytic activity. This activated complex then cleaves  
30 soluble complement proteins C4 and C2 into C4a, C4b, C2a and C2b, respectively. The  
31 C4a and C2b fragments bind to form the C4bC2a protease, which is also known as the  
32 classical C3 convertase. The lectin pathway is initiated through the binding of L-ficolin or  
33 Mannose Binding Lectin (MBL) to carbohydrates on the surfaces of bacterial pathogens.  
34 These complexes, in combination with the associated mannose-associated serine pro-  
35 teases 1 and 2 (MASP-1/2), also cleave C4 and C2, leading to additional classical C3  
36 convertase. Thus, the classical and lectin pathways, initiated by the recognition of a for-  
37 eign surface, converge at the classical C3 convertase. However, the alternate pathway  
38 works differently. The alternate pathway involves a 'tickover' mechanism in which com-  
39 plement protein C3 is spontaneously hydrolyzed to form an activated intermediate C3w;  
40 C3w recruits factor B and factor D, leading to the formation of C3wBb. C3wBb can cleave  
41 C3 into C3a and C3b, where the C3b fragment can further recruit additional factor B and  
42 factor D to form C3bBbC3b, which is also known as the alternate C3 convertase (9). The  
43 role of classical and alternate C3 convertases is varied. First, C3 convertases encode  
44 an amplification loop by cleaving C3 into C3a and C3b; the C3b fragment is then free to  
45 form additional alternate C3 convertases, thereby forming a positive feedback loop. Next,  
46 C3 convertase activity links complement initiation with the terminal phase of the cascade  
47 through the formation of C5 convertases. Both classical and alternate C3 convertases can  
48 recruit an additional C3b subunit to form the classical C5 convertase (C4bC2aC3b), and  
49 the alternate C5 convertase (C3bBbC3b), respectively. C5 convertases cleave C5 into  
50 the C5a and C5b fragments. The C5b fragment, along with the C6, C7, C8 and multiple  
51 C9 complement proteins, form the membrane attack complex. On the other hand, both  
52 C3a and C5a are important inflammatory signals involved in several responses (7, 8).

Activation of the complement cascade is strongly regulated by many plasma and host cell proteins. The initiation of the classical pathway via complement protein C1 is controlled by the C1 Inhibitor (C1-Inh), a protease inhibitor belonging to the serpin superfamily. C1-Inh irreversibly binds to and deactivates the active subunits of C1, preventing spontaneous fluid phase and chronic activation of complement (10). Regulation of the upstream elements of complement is also achieved through the interaction of the C4 binding protein (C4BP) with C4b, as well as through the interaction of factor H with C3b (11). These regulatory proteins are also capable of binding their respective targets while they are bound in convertase complexes. Membrane cofactor protein (MCP or CD46) possesses a cofactor activity for C4b and C3b, which protects the host from self-activation of complement (12). Decay accelerating factor (DAF or CD55) is also able to recognize and dissociate both C3 and C5 convertases (13). Carboxypeptidase-N, a well known inflammation regulator, cleaves carboxyl-terminal arginines and lysines of the complement proteins C3a, C4a, and C5a rendering them inactive (14). Lastly, the assembly of the MAC complex is inhibited by vitronectin and clusterin in the plasma, and CD59 at the host surface (15, 16). Thus, there are many points of control which influence complement activation across the three activation pathways.

Developing quantitative mathematical models of complement could be crucial to understanding its role in the body. Traditionally, complement models have been formulated as systems of linear or non-linear ordinary differential equations (ODEs). For example, Hirayama et al. modeled the classical complement pathway as a system of linear ODEs (17), while Korotaevskiy and co-workers modeled the classical, lectin and alternate pathways as a system of non-linear ODEs (18). More recently, large mechanistic models of sections of complement have also been proposed. For example, Liu et al. analyzed the formation of the classical and lectin C3 convertases, and the regulatory role of C4BP using a system of 45 non-linear ODEs with 85 parameters (19). Recently, Zewde and co-

79 workers constructed a detailed mechanistic model of the alternative pathway which con-  
80 sisted of 107 ODEs and 74 kinetic parameters and delineated the complement response  
81 of the host and pathogen (16). However, these previous modeling studies involved little  
82 experimental validation. Thus, while these models are undoubtably important theoretical  
83 tools, it is unclear if they can describe or quantitatively predict experimentally validated  
84 complement dynamics. The central challenge is the estimation of model parameters from  
85 experimental data. Unlike other important cascades, such as coagulation for which there  
86 are well developed experimental tools and many publicly available data sets, the data for  
87 complement is relatively sparse. Missing or incomplete data sets, and limited quantitative  
88 data make the identification of mechanistic complement models difficult.

89 In this study, we developed an ensemble of experimentally validated reduced order  
90 complement models. The modeling approach combined ordinary differential equations  
91 with logical rules to produce a complement model with a limited number of equations and  
92 parameters. The reduced order model, which described the lectin and alternative path-  
93 ways, consisted of 18 differential equations with 28 parameters. Thus, the model was an  
94 order of magnitude smaller and included more pathways than comparable mathematical  
95 models in the literature. We estimated an ensemble of model parameters from *in vitro*  
96 time series measurements of the C3a and C5a complement proteins. Subsequently, we  
97 validated the model on unseen C3a and C5a measurements that were not used for model  
98 training. Despite its small size, the model was surprisingly predictive. After validation, we  
99 performed global sensitivity and robustness analysis to estimate which parameters and  
100 species controlled model performance. These analyses suggested complement was ro-  
101 bust to any single therapeutic intervention. The only intervention that consistently reduced  
102 C5a formation for all cases was a dual-knockdown of both C3 and C5. Taken together,  
103 we developed a reduced order complement model that was computationally inexpensive,  
104 and could easily be incorporated into pre-existing or new pharmacokinetic models of im-

<sup>105</sup> immune system function. The model described experimental data, and predicted the need  
<sup>106</sup> for multiple points of intervention to disrupt complement activation.

107 **Results**

108 **Reduced order complement network.** The complement model described the alternate  
109 and lectin pathways (Fig. 1). A trigger event initiated the lectin pathway, which activated  
110 the cleavage of C2 and C4 into C2a, C2b, C4a and C4b respectively. Classical Pathway  
111 (CP) C3 convertase (C4aC2b) then catalyzed the cleavage of C3 into C3a and C3b. The  
112 alternate pathway was initiated through the spontaneous hydrolysis of C3 into C3a and  
113 C3b (not C3w). The C3b fragment generated by hydrolysis (or by CP C3 convertase)  
114 could then form the alternate pathway (AP) C3 convertase (C3bBb). We did not consider  
115 C3w, nor the formation of the initial alternate C3 convertase (C3wBb). Rather, we as-  
116 sumed C3w was equivalent to C3b and only modeled the formation of the main AP C3  
117 convertase. Both the CP and AP C3 convertases catalyzed the cleavage of C3 into C3a  
118 and C3b. A second C3b fragment could then bind with either the CP or AP C3 convertase  
119 to form the CP or AP C5 convertase (C4bC2aC3b or C3bBbC3b). Both C5 convertases  
120 catalyzed the cleavage of C5 into the C5a and C5b fragments. In this initial study, we  
121 simplified the model by assuming both Factor B and Factor D were in excess. However,  
122 we did explicitly account for two control proteins, Factor H and C4BP. Lastly, we did not  
123 consider MAC formation, instead we stopped at C5a and C5b. Lectin pathway activation,  
124 and C3/C5 convertase activity was modeled using a combination of saturation kinetics  
125 and non-linear transfer functions, which facilitated a significant reduction in the size of the  
126 model while maintaining performance. Binding interactions were modeled using mass-  
127 action kinetics, where we assumed all binding was irreversible. Thus, while the reduced  
128 order complement model encoded significant biology, it was highly compact consisting of  
129 only 18 differential equations and 28 model parameters. Next, we estimated an ensemble  
130 of model parameters from time series measurements of the C3a and C5a complement  
131 proteins.

132 **Estimating an ensemble of reduced order complement models.** A critical challenge  
133 for the development of any dynamic model is the estimation of model parameters. We  
134 estimated an ensemble of complement model parameters in a hierarchical fashion using  
135 *in vitro* time-series data sets generated with and without zymosan, a lectin pathway acti-  
136 vator (20). The residual between model simulations and experimental measurements was  
137 minimized using the dynamic optimization with particle swarms (DOPS) routine, starting  
138 from an initial random parameter guess. Unless otherwise specified, all initial conditions  
139 were assumed to be their mean physiological values. A hierarchical approach was taken  
140 in which the alternate pathway parameters were estimated first and then fixed during the  
141 estimation of the lectin pathway parameters. While we had significant training data, the  
142 parameter estimation problem was underdetermined (we were not able to uniquely deter-  
143 mine model parameters). Thus, instead of using a best-fit yet uncertain parameter set, we  
144 estimated an ensemble of probable parameter sets ( $N = 50$ , see materials and methods).  
145 The reduced order complement model ensemble captured the behavior of both the alter-  
146 native and lectin pathways (Fig. 2). For the alternative pathway, we used C3a and C5a  
147 measurements in the absence of zymosan, and only allowed the alternative parameters  
148 to vary (Fig. 2A and B). On the other hand, lectin pathway parameters were estimated  
149 from C3a and C5a measurements in the presence of 1g zymosan with alternate pathway  
150 parameters fixed (Fig. 2C and D). The reduced order model reproduced a panel of alter-  
151 nate and lectin pathway data sets in the neighborhood of physiological factor and inhibitor  
152 concentrations. However, it was unclear whether the reduced order model could predict  
153 new data, without updating the model parameters. To address this question, we fixed the  
154 model parameters and simulated data sets not used for model training.

155 We tested the predictive power of the reduced order complement model with data  
156 not used during model training (Fig. 3). Six validation cases were considered, three for  
157 C3a and C5a, respectively. All model parameters and initial conditions were fixed for the

validation simulations (with the exception of zymosan). The ensemble of reduced order models predicted the qualitative dynamics of C3a formation (Fig. 3, left column), and C5a formation (Fig. 3, right column) at three inducer concentrations. However, there were shortcomings with model performance, especially for the C3a prediction. First, while the overall C3a trend was captured, the level of C3a was consistently under-predicted (outside of our 99% confidence interval) in all cases (Fig. 3, left column). We believe the C3a under-prediction was related to our choice of training data, and how we modeled C4BP interactions. We trained the model using 1g zymosan, but predicted cases with much less initiator. Next, the C4BP interactions were modeled as irreversible binding steps resulting in completely inactive complexes. However, the binding of C4BP with complement proteins is likely reversible, and CP C3 convertase may have residual activity even in the bound form. Thus, the model likely over-predicted the influence of C4BP. Second, while the C5a measurements were within the 99% confidence estimate, we failed to capture the concave down curvature for the 0.001g and 0.01g zymosan cases. The decreasing slope of the C5a may indicate cofactor limitation, or missing biology which we have not accounted for in the reduced order approach. Despite these shortcomings, we qualitatively predicted unseen experimental data, including correctly capturing the time scale of C3a formation, and the correct order of magnitude for C5a for three inducer levels. Next, we used global sensitivity and robustness analysis to determine which parameters and species controlled the performance of the complement model.

**Global analysis of the reduced order complement model.** We conducted sensitivity analysis to estimate which parameters controlled the performance of the reduced order complement model. We calculated the sensitivity of the C3a and C5a residuals to changes in model parameters with and without zymosan for the ensemble of parameter sets (Fig. 4A - D). In the absence of zymosan (where only the alternative pathway is active),  $k_{f,C3b}$  (tickover formation of C3b) and  $k_{d,C3a}$  (rate constant governing C3a degra-

dation) controlled the C3a fit (Fig. 4A). Interestingly, neither  $k_{c,C3C,AP}$  (the rate constant governing AP C3-convertase activity) nor  $k_{f,C3C,AP}$  (the rate constant governing AP C3-convertase formation) were sensitive in the absence of zymosan. Thus, C3a formation in the alternative pathway was more heavily influenced by the spontaneous hydrolysis of C3, rather than AP C3-convertase activity, in the absence of zymosan. On the other hand, the C5a residual was strongly sensitive to tickover parameters e.g.,  $k_{f,C3b}$ , and to a lesser extent  $k_{f,C3C,AP}$  as well as parameters controlling AP C5 convertase activity in the absence of zymosan (Fig. 4B). Thus, AP C3-convertase did not influence C3a dynamics, but strongly effected C5a formation in the absence of zymosan. In the presence of zymosan, the C3a residual was controlled by the formation and activity of the CP C3 convertase, as well as tickover and degradation parameters (Fig. 4C). Further, the C5a residual was influenced by lectin initiation parameters, the formation and activity of CP C5 convertase, and the inhibition by C4BP in the presence of zymosan (Fig. 4D). Globally, sensitivity analysis suggested that lectin pathway parameters dominated system performance in the presence of zymosan, and that C5a formation was sensitive to both C3 and C5 convertase activity, while C3a was robust to the AP C3 convertase. In the absence of zymosan, the tickover parameters were important to both C3a and C5a formation, but C5a was also sensitive to both AP C3 and C5 convertase formation. We compared the sensitivity results to current therapeutic approaches; pathways involving sensitive parameters have been targeted for clinical intervention (Fig. 4E). Thus, there was a qualitative overlap between sensitivity and the potential of biochemical efficacy. However, sensitivity coefficients are only a local measure of how small changes in a parameters affect model performance. To more closely simulate a clinical intervention e.g., administration of an anti-complement inhibitor, we performed robustness analysis.

Robustness coefficients quantify the response of a marker to a macroscopic structural or operational perturbation to a biochemical network. Here, we computed how the C3a

and C5a trajectories responded to a decrease in the initial abundance of C3 and/or C5. Robustness analysis suggested there was no single intervention that inhibited complement activation in the presence of both initiation pathways (Fig. 5). We calculated robustness indices for C3a and C5a for the parameter ensemble ( $N = 50$ ) with and without the lectin pathway initiator. We simulated the addition of different doses of anti-complement inhibitor cocktails by decreasing the initial concentration of C3 or C5 or the combination of C3 and C5 by 50% and 90%. This would be conceptually analogous to the administration of a C3 inhibitor e.g., compstatin alone or combination with eculizumab (Fig. 4E). A  $\log_{10}$  transformed robustness index of zero indicated no effect due to the perturbation, whereas an index of less than zero indicated decreased C3a or C5a. The response of the complement model to different knock-down magnitudes was non-linear; a 90% knock-down had an order of magnitude more impact than a 50% knock-down. As expected, a C5 knock-down had no effect on C3a formation for either the alternate (Fig. 5A, lanes 1 or 3) or lectin pathways (Fig. 5B, lanes 1 or 3). However, C3a abundance and to a lesser extent C5a abundance decreased with decreasing C3 concentration in the alternate pathway (Fig. 5A or B, lanes 1 or 2). This agreed with the sensitivity results; changes in AP C3-convertase formation affected the downstream dynamics of C5a formation. Thus, if we only considered the alternate pathway, C3 alone could be a reasonable target, especially given that C5a formation was surprisingly robust to C5 levels in the alternate pathway (Fig. 5A or B, lane 2). Yet, when both pathways were activated, C5a levels were robust to the initial C3 concentration (Fig. 5A or B, lane 4); C5a formation was catalyzed by CP C3 and C5 convertases. Thus, the only reliable intervention that consistently reduced both C3a and C5a formation for all cases was a dual-knockdown of C3 and C5. For example, a 90% decrease of both C3 and C5 reduced the formation of C5a by over an order of magnitude (Fig. 5B, lane 4), while C3a was reduced to a lesser extent (Fig. 5B, lane 3).

235 **Discussion**

236 In this study, we developed an ensemble of experimentally validated reduced order com-  
237 plement models. The modeling approach combined ordinary differential equations with  
238 logical rules to produce a complement model with a limited number of equations and pa-  
239 rameters. The reduced order model, which described the lectin and alternative pathways,  
240 consisted of 18 differential equations with 28 parameters. Thus, the model was an order  
241 of magnitude smaller and included more pathways than comparable mathematical mod-  
242 els in the literature. We estimated an ensemble of model parameters from *in vitro* time  
243 series measurements of the C3a and C5a complement proteins. Subsequently, we val-  
244 idated the model on unseen C3a and C5a measurements that were not used for model  
245 training. Despite its small size, the model was surprisingly predictive. After validation, we  
246 performed global sensitivity and robustness analysis to estimate which parameters and  
247 species controlled model performance. These analyses suggested complement was ro-  
248 bust to any single therapeutic intervention. The only intervention that consistently reduced  
249 C5a formation for all cases was a dual-knockdown of both C3 and C5. Taken together,  
250 we developed a reduced order complement model that was computationally inexpensive,  
251 and could easily be incorporated into pre-existing or new pharmacokinetic models of im-  
252 mune system function. The model described experimental data, and predicted the need  
253 for multiple points of intervention to disrupt complement activation.

254 Despite its importance, there has been a paucity of validated mathematical models  
255 of complement pathway activation. To our knowledge, this study is one of the first com-  
256 plement models that combined multiple initiation pathways with experimental validation  
257 of important complement products like C5a. However, there have been several theoreti-  
258 cal models of components of the cascade in the literature. Liu and co-workers modeled  
259 the formation of C3a through the classical pathway using 45 non-linear ODEs (19). In  
260 contrast, in this study we modeled lectin mediated C3a formation using only five ODEs.

Though we did not model all the initiation interactions in detail, especially the cross-talk between the lectin and classical pathways, we successfully captured C3a dynamics with respect to different concentrations of lectin initiators. The model also captured the dynamics of C3a and C5a formed from the alternate pathway using only seven ODEs. The reduced order model predictions of C5a were qualitatively similar to the theoretical complement model of Zewde et al which involved over 100 ODEs (16). However, we found that the quantity of C3a produced in the alternate pathway was nearly 1000 times the quantity of C5a produced. Though this was in agreement with the experimental data (20), it differed from the theoretical predictions made by Zewde et al. who showed C3a was  $10^8$  times the C5a concentration (16). In our model, the time profile of C5a generation from the lectin pathway changed with respect to the quantity of zymosan (the lectin pathway initiator). The lag phase for generation was inversely proportional to the initiator concentration. Korotaevskiy et al. showed a similar trend using a theoretical model of complement, albeit for much shorter time scales (18). Thus, the reduced order complement model performed similarly to existing large mechanistic models, despite being significantly smaller.

Global analysis of the complement model estimated potential important therapeutic targets. Complement malfunctions are implicated in a number of diseases, however the development of complement specific therapeutics has been challenging (3, 21). Previously, we have shown that mathematical modeling and sensitivity analysis can be useful tools to estimate therapeutically important mechanisms in biochemical networks (22–25). In this study, we analyzed a validated ensemble of reduced order complement models to estimate therapeutically important mechanisms. In presence of an initiator, C5a formation was primarily sensitive to the lectin initiation parameters, and parameters governing the conversion of C5 to C5a and C5b. This result agrees well with the current protease inhibitors targeting initiating complexes, including mannose-associated serine proteases 1 and 2 (MASP-1,2) (26). The most commonly used anti-complement drug eculizumab

287 (21), targets the C5 protein which is cleaved to form C5a. Our sensitivity analysis showed  
288 that kinetic parameters governing C5 conversion were sensitive in both lectin initiated and  
289 alternate pathways, thus agreeing with targeting C5 protein. The formation of basal C3b  
290 was also a sensitive parameter in the formation of C3a through the alternate pathway.  
291 Thus, this mechanism can act as a target for both C3a and C5a inhibitors. Lectin initiated  
292 C3a formation showed a number of sensitive parameters. This included the lectin initi-  
293 ation parameters that controlled C5a formation, C3 convertase inhibition by C4BP, and  
294 parameters governing C3 convertase activity. All these mechanisms are potential drug  
295 targets.

296 To further validate these results from sensitivity analysis about potential drug targets  
297 we did a robustness analysis. We knocked down C3 and C5 levels and studied their im-  
298 pact on the generation of C3a and C5a. The C3a and C5a levels in the lectin pathway  
299 were strongly influenced by initial levels of C3 and C5. Thus direct inhibition of C3 and  
300 C5, or targeting complexes (MASP complex, C3 and C5 convertases) that act on C3 and  
301 C5 have a direct impact on production of C3a and C5a. This is also in agreement with  
302 sensitivity analysis that C5 is a good drug target. A number of drugs targeting C5 are  
303 being developed. For example LFG316 by Novartis is being used to target C5 in cases  
304 of Age-Related Macular Degeneration (27), Mubodina is an antibody that targets C5 in  
305 the treatment of Atypical Hemolytic-Uremic Syndrome (aHUS) (28), Coversin is a small  
306 molecule targeting C5 (29), Zimura is an aptamer targeting C5 (30), small peptides and  
307 RNAi are also being used to inhibit C5 (31). Another important conclusion that can be  
308 drawn together from sensitivity and robustness analysis is that C3 and C5 convertases  
309 can be important therapeutic targets. Though knockdown of C3 and C5 affects C3a and  
310 C5a levels downstream, the abundance and turnover rate (32, 33) of these proteins make  
311 them difficult targets. Thus targeting C3 and C5 directly will require high dosage of drugs.  
312 It is also well known that eculizumab dosage needs to be adjusted while treating for Atyp-

313      ical Hemolytic-Uremic Syndrome (aHUS), a disease that is caused due to uncontrolled  
314      complement activation (34). The issue of high dosage can potentially be circumvented  
315      by targeting convertases or fragile mechanisms that involve C3, C5 or their activated  
316      components. Our analysis shows that formation and assembly of these convertases are  
317      sensitive mechanisms that strongly impact downstream proteins like C5a. Formation of  
318      convertases is inhibited by targeting upstream protease complexes like MASP-1,2 from  
319      lectin pathway (or C1r, C1s from classical pathway). For example, Omeros is a protease  
320      inhibitor that targets MASP-2 complex and thereby inhibits formation of downstream con-  
321      vertases (35). Lampalizumab (an immunoglobulin) and Bikaciomab (an antibody frag-  
322      ment) target Factor B and Factor D respectively. Factor B and Factor D are crucial to  
323      formation alternate pathway convertases (36, 37). Novelmed Therapeutics recently de-  
324      veloped antibody, NM9401 against propedin, a small protein that stabilizes alternate C3  
325      convertase (38). Cobra Venom Factor (CVF), an analogue of C3b has been used to bind  
326      to Factor B to regulate alternate convertases (39). Thus, analysis of the ensemble of com-  
327      plement models identified potentially important therapeutic targets that are consistent with  
328      therapeutic strategies that are under development.

329      The performance of the complement model was impressive given its limited size. How-  
330      ever, there are several questions that should be explored further. A logical progression for  
331      this work would be to expand the network to include the classical pathway and the forma-  
332      tion of the membrane attack complex (MAC). However, it is unclear whether the addition  
333      of the classical pathway will decrease the predictive quality of our existing model. Liu  
334      et al have shown cross-talk between the activation of the classical and lectin pathways  
335      that could influence model performance (19). One potential approach to address such  
336      difficulties would be to incorporate C reactive proteins (CRP) and L-ficolin (LF) into the  
337      model, both of which are involved with the initiation of classical and lectin pathways. Liu  
338      et al. showed that under inflammation conditions interactions between lectin and classical

pathways was mediated through CRP and LF (19). Thus incorporating these two proteins would help us in modeling cross talk. Time course measurements of MAC abundance (and MAC formation dynamics) are also scarce, making the inclusion of MAC challenging. Next, we should address the under-prediction of C3a. We believe the C3a under-prediction can be attributed to how we modeled C4BP interactions. C4BP interactions were modeled as irreversible binding steps resulting in completely inactive complexes; however, the binding of C4BP with complement proteins is likely reversible and C4BP-bound convertases may have residual activity. We also did not capture the maximum concentration of C3a at low initiator levels. One possible reasons for this could be the C2-by-pass pathway, which was not included in the model. This pathway further accelerates C3a production without the involvement of a C3 convertase. Currently the C3a in the model is generated only through the activity of a C3 convertase. Incorporating this additional step within the reduced order modeling framework would be a future direction that we need to consider. We should test alternative model structures which include reversible C4BP binding, and partially active convertases. Alternatively, we could also perform sensitivity analysis on the C3a prediction residual to determine which parameters controlled the C3a prediction.

356 **Materials and Methods**

357 **Formulation and solution of the complement model equations.** We used ordinary  
 358 differential equations (ODEs) to model the time evolution of complement proteins ( $x_i$ ) in  
 359 the reduced order model:

$$\frac{dx_i}{dt} = \sum_{j=1}^{\mathcal{R}} \sigma_{ij} r_j(\mathbf{x}, \epsilon, \mathbf{k}) \quad i = 1, 2, \dots, \mathcal{M} \quad (1)$$

360 where  $\mathcal{R}$  denotes the number of reactions and  $\mathcal{M}$  denotes the number of protein species  
 361 in the model. The quantity  $r_j(\mathbf{x}, \epsilon, \mathbf{k})$  denotes the rate of reaction  $j$ . Typically, reaction  $j$  is  
 362 a non-linear function of biochemical and enzyme species abundance, as well as unknown  
 363 model parameters  $\mathbf{k}$  ( $\mathcal{K} \times 1$ ). The quantity  $\sigma_{ij}$  denotes the stoichiometric coefficient for  
 364 species  $i$  in reaction  $j$ . If  $\sigma_{ij} > 0$ , species  $i$  is produced by reaction  $j$ . Conversely, if  $\sigma_{ij} < 0$ ,  
 365 species  $i$  is consumed by reaction  $j$ , while  $\sigma_{ij} = 0$  indicates species  $i$  is not connected  
 366 with reaction  $j$ . Species balances were subject to the initial conditions  $\mathbf{x}(t_0) = \mathbf{x}_0$ .

367 Rate processes were written as the product of a kinetic term ( $\bar{r}_j$ ) and a control term  
 368 ( $v_j$ ) in the complement model. The kinetic term for the formation of C4a, C4b, C2a and  
 369 C2b, lectin pathway activation, and C3 and C5 convertase activity was given by:

$$\bar{r}_j = k_j^{max} \epsilon_i \left( \frac{x_s^\eta}{K_{js}^\eta + x_s^\eta} \right) \quad (2)$$

370 where  $k_j^{max}$  denotes the maximum rate for reaction  $j$ ,  $\epsilon_i$  denotes the abundance of the  
 371 enzyme catalyzing reaction  $j$ ,  $\eta$  denotes a cooperativity parameter, and  $K_{js}$  denotes the  
 372 saturation constant for species  $s$  in reaction  $j$ . We used mass action kinetics to model  
 373 protein-protein binding interactions within the network:

$$\bar{r}_j = k_j^{max} \prod_{s \in m_j^-} x_s^{-\sigma_{sj}} \quad (3)$$

<sup>374</sup> where  $k_j^{max}$  denotes the maximum rate for reaction  $j$ ,  $\sigma_{sj}$  denotes the stoichiometric coefficient for species  $s$  in reaction  $j$ , and  $s \in m_j$  denotes the set of *reactants* for reaction  $j$ .  
<sup>375</sup> We assumed all binding interactions were irreversible.

<sup>377</sup> The control terms  $0 \leq v_j \leq 1$  depended upon the combination of factors which influenced rate process  $j$ . For each rate, we used a rule-based approach to select from competing control factors. If rate  $j$  was influenced by  $1, \dots, m$  factors, we modeled this relationship as  $v_j = \mathcal{I}_j(f_{1j}(\cdot), \dots, f_{mj}(\cdot))$  where  $0 \leq f_{ij}(\cdot) \leq 1$  denotes a regulatory transfer function quantifying the influence of factor  $i$  on rate  $j$ . The function  $\mathcal{I}_j(\cdot)$  is an integration rule which maps the output of regulatory transfer functions into a control variable. Each regulatory transfer function took the form:

$$f_{ij}(\mathcal{Z}_i, k_{ij}, \eta_{ij}) = k_{ij}^{\eta_{ij}} \mathcal{Z}_i^{\eta_{ij}} / (1 + k_{ij}^{\eta_{ij}} \mathcal{Z}_i^{\eta_{ij}}) \quad (4)$$

<sup>384</sup> where  $\mathcal{Z}_i$  denotes the abundance of factor  $i$ ,  $k_{ij}$  denotes a gain parameter, and  $\eta_{ij}$  denotes  
<sup>385</sup> a cooperativity parameter. In this study, we used  $\mathcal{I}_j \in \{min, max\}$  (40). If a process has  
<sup>386</sup> no modifying factors,  $v_j = 1$ . The model equations were implemented in MATLAB and  
<sup>387</sup> solved using the ODE23s routine (The Mathworks, Natick MA). The complement model  
<sup>388</sup> code and parameter ensemble is freely available under an MIT software license and can  
<sup>389</sup> be downloaded from <http://www.varnerlab.org>.

<sup>390</sup> **Estimation of an ensemble of complement model parameters.** We minimized the  
<sup>391</sup> residual between simulations and experimental C3a and C5a measurements using Dy-  
<sup>392</sup> namic Optimization with Particle Swarms (DOPS). DOPS minimized the objective:

$$\min_{\mathbf{k}} \sum_{\tau=1}^{\mathcal{T}} \sum_{j=1}^S \left( \frac{\hat{x}_j(\tau) - x_j(\tau, \mathbf{k})}{\omega_j(\tau)} \right)^2 \quad (5)$$

393 where  $\hat{x}_j(\tau)$  denotes the measured value of species  $j$  at time  $\tau$ ,  $x_j(\tau, \mathbf{k})$  denotes the sim-  
 394 ulated value for species  $j$  at time  $\tau$ , and  $\omega_j(\tau)$  denotes the experimental measurement  
 395 variance for species  $j$  at time  $\tau$ . The outer summation is with respect to time, while the  
 396 inner summation is with respect to state. DOPS is a novel metaheuristic that combines  
 397 multi swarm particle swarm optimization (PSO) with a greedy global optimization algo-  
 398 rithm called dynamically dimensioned search (DDS). DOPS is faster than conventional  
 399 global optimizers and has the ability to find near optimal solutions for high dimensional  
 400 systems within a relatively few function evaluations. It uses an adaptive switching strat-  
 401 egy based on error convergence rates to switch from the particle swarm to DDS search  
 402 phases. This enables DOPS to quickly estimate globally optimal or near optimal solutions  
 403 even in the presence of many local minima. In the swarm search, for each iteration the  
 404 particles compute error within each sub-swarm by evaluating the model equations using  
 405 their specific parameter vector realization. From each of these points within a sub-swarm  
 406 a local best is identified. This along with the particle best within the sub-swarm  $S_k$  is used  
 407 to update the parameter estimate for each particle using the following rules:

$$z_{i,j} = \theta_{1,j-1} z_{i,j-1} + \theta_2 r_1 (\mathcal{L}_i - z_{i,j-1}) + \theta_3 r_2 (\mathcal{G}_k - z_{i,j-1}) \quad (6)$$

408 where  $z_{i,j}$  is the parameter vector,  $(\theta_1, \theta_2, \theta_3)$  were adjustable parameters,  $\mathcal{L}_i$  denotes the  
 409 best solution found by particle  $i$  within sub-swarm  $S_k$  for function evaluations  $1 \rightarrow j-1$ , and  
 410  $\mathcal{G}_k$  denotes the best solution found over all particles within sub-swarm  $S_k$ . The quantities  
 411  $r_1$  and  $r_2$  denote uniform random vectors with the same dimension as the number of  
 412 unknown model parameters ( $\mathcal{K} \times 1$ ). At the conclusion of the swarm phase, the overall  
 413 best particle,  $\mathcal{G}_k$ , over the  $k$  sub-swarms was used to initialize the DDS phase. For the

414 DDS phase, the best parameter estimate was updated using the rule:

$$\mathcal{G}_{new}(J) = \begin{cases} \mathcal{G}(J) + \mathbf{r}_{normal}(J)\sigma(J), & \text{if } \mathcal{G}_{new}(J) < \mathcal{G}(J). \\ \mathcal{G}(J), & \text{otherwise.} \end{cases} \quad (7)$$

415 where  $J$  is a vector representing the subset of dimensions that are being perturbed,  $\mathbf{r}_{normal}$   
416 denotes a normal random vector of the same dimensions as  $\mathcal{G}$ , and  $\sigma$  denotes the pertur-  
417 bation amplitude:

$$\sigma = R(\mathbf{p}^U - \mathbf{p}^L) \quad (8)$$

418 where  $R$  is the scalar perturbation size parameter,  $\mathbf{p}^U$  and  $\mathbf{p}^L$  are  $(\mathcal{K} \times 1)$  vectors that  
419 represent the maximum and minimum bounds on each dimension. The set  $J$  was con-  
420 structed using a monotonically decreasing probability function  $\mathcal{P}_i$  that represents a thresh-  
421 old for determining whether a specific dimension  $j$  was perturbed or not. DDS updates  
422 are greedy;  $\mathcal{G}_{new}$  becomes the new solution vector only if it is better than  $\mathcal{G}$ . At the end of  
423 DDS phase we obtain the optimal vector  $\mathcal{G}$  which we use for plotting best fits against the  
424 experimental data, and for generating a parameter ensemble.

425 An ensemble of parameters was obtained by randomly perturbing the optimal param-  
426 eter set within bounds established by analyzing repeated DOPS runs. Parameters were  
427 selected using goodness of fit (model residual) and numerical stability criteria. We se-  
428 lected an ensemble of  $N = 50$  parameter sets for this study using this sampling proce-  
429 dure. The best fit parameter set, and parameter ensemble is available in a tab delim-  
430 ited plain text format from the Complement model GitHub repository. The DOPS routine  
431 was implemented in MATLAB (The Mathworks, Natick MA) and can be downloaded from  
432 <http://www.varnerlab.org> under an MIT software license.

433 **Sensitivity and robustness analysis of complement model performance.** We con-  
434 ducted global sensitivity and robustness analysis to estimate which parameters and species

435 controlled the performance of the reduced order model. We computed the total variance-  
 436 based sensitivity index of each parameter relative to the training residual for the C3a  
 437 alternate, C5a alternate, C3a lectin, and C5a lectin cases using the Sobol method (41).  
 438 The sampling bounds for each parameter were established from the minimum and maxi-  
 439 mum value for that parameter in the parameter ensemble. We used the sampling method  
 440 of Saltelli *et al.* to compute a family of  $N(2d + 2)$  parameter sets which obeyed our pa-  
 441 rameter ranges, where  $N$  was the number of trials per parameters, and  $d$  was the number  
 442 of parameters in the model (42). In our case,  $N = 200$  and  $d = 28$ , so the total sensitivity  
 443 indices were computed using 11,600 model evaluations. The variance-based sensitivity  
 444 analysis was conducted using the SALib module encoded in the Python programming  
 445 language (43).

446 Robustness coefficients quantify the response of a marker to a structural or operational  
 447 perturbation to the network architecture. Robustness coefficients were calculated as  
 448 shown previously (44). Log-transformed robustness coefficients denoted by  $\hat{\alpha}(i, j, t_o, t_f)$   
 449 are defined as:

$$\hat{\alpha}(i, j, t_o, t_f) = \log_{10} \left[ \left( \int_{t_o}^{t_f} x_i(t) dt \right)^{-1} \left( \int_{t_o}^{t_f} x_i^{(j)}(t) dt \right) \right] \quad (9)$$

450 Here  $t_o$  and  $t_f$  denote the initial and final simulation time, while  $i$  and  $j$  denote the indices  
 451 for the marker and the perturbation, respectively. A value of  $\hat{\alpha}(i, j, t_o, t_f) > 0$ , indicates  
 452 increased marker abundance, while  $\hat{\alpha}(i, j, t_o, t_f) < 0$  indicates decreased marker abun-  
 453 dance following perturbation  $j$ . If  $\hat{\alpha}(i, j, t_o, t_f) \sim 0$ , perturbation  $j$  did not influence the  
 454 abundance of marker  $i$ . In this study, we perturbed the initial condition of C3 or C5 or  
 455 a combination of C3 and C5 by 50% or 90% and measured the area under the curve  
 456 (AUC) of C3a or C5a with and without lectin initiator. Log-transformed robustness coeffi-  
 457 cients were calculated for every member of the ensemble, where the mean  $\pm 1 \times$  standard-

<sup>458</sup> deviation are reported.

459 **Competing interests**

460 The authors declare that they have no competing interests.

461 **Author's contributions**

462 J.V directed the study. A.S developed the reduced order complement model and the  
463 parameter ensemble. A.S, W.D and M.M analyzed the model ensemble, and generated  
464 figures for the manuscript. The manuscript was prepared and edited for publication by  
465 A.S, W.D, M.M and J.V.

466 **Acknowledgements**

467 We gratefully acknowledge the suggestions from the anonymous reviewers to improve  
468 this manuscript.

469 **Funding**

470 This study was supported by an award from the US Army and Systems Biology of Trauma  
471 Induced Coagulopathy (W911NF-10-1-0376) to J.V. for the support of A.S.

472 **References**

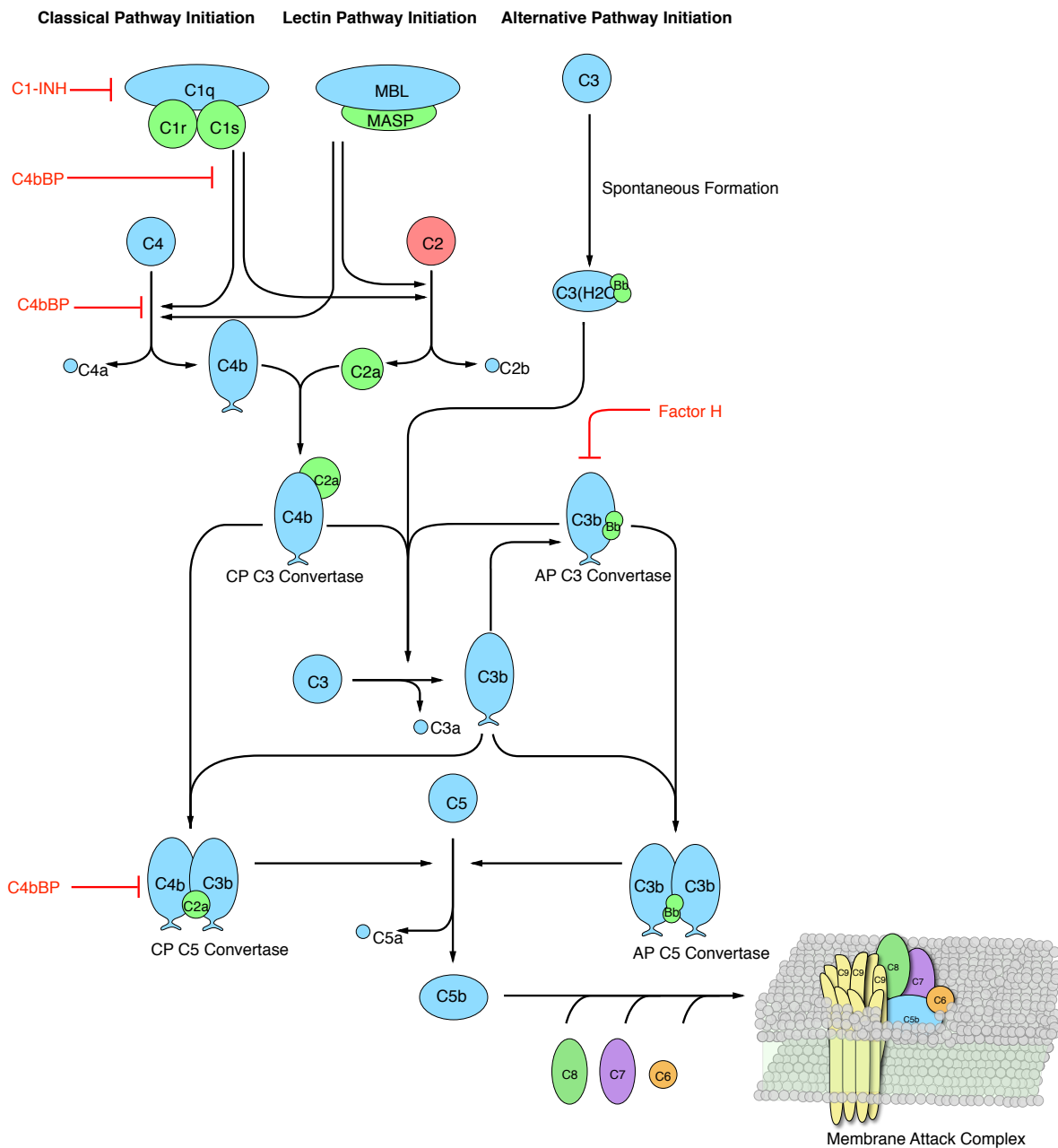
- 473 1. Nuttall G (1888) Experimente über die bacterienfeindlichen Einflüsse des thierischen  
474 Körpers. Z Hyg Infektionskr 4: 353-394.
- 475 2. Ricklin D, Hajishengallis G, Yang K, Lambris JD (2010) Complement: a key system  
476 for immune surveillance and homeostasis. NAT IMMUNOL 11: 785–797.
- 477 3. Ricklin D, Lambris JD (2007) Complement-targeted therapeutics. NAT BIOTECHNOL  
478 25: 1265-1275.
- 479 4. Rittirsch D, Flierl MA, Ward PA (2008) Harmful molecular mechanisms in sepsis. NAT  
480 REV IMMUNOL 8: 776–787.
- 481 5. Sarma JV, Ward PA (2011) The complement system. Cell Tissue Res 343: 227–235.
- 482 6. Ricklin D, Lambris JD (2013) Complement in immune and inflammatory disorders:  
483 pathophysiological mechanisms. J Immunol 190: 3831–3838.
- 484 7. Walport MJ (2001) Complement. first of two parts. N Engl J Med 344: 1058-66.
- 485 8. Walport MJ (2001) Complement. second of two parts. N Engl J Med 344: 1140-4.
- 486 9. Pangburn MK, Müller-Eberhard HJ (1984) The alternative pathway of complement.  
487 Semin Immunopathol .
- 488 10. Walker D, Yasuhara O, Patston P, McGeer E, McGeer P (1995) Complement c1 in-  
489 hibitor is produced by brain tissue and is cleaved in alzheimer disease. Brain Res  
490 675: 75–82.
- 491 11. Blom AM, Kask L, Dahlbäck B (2001) Structural requirements for the complement  
492 regulatory activities of c4bp. J Biol Chem 276: 27136–27144.
- 493 12. Riley-Vargas RC, Gill DB, Kemper C, Liszewski MK, Atkinson JP (2004) Cd46: ex-  
494 panding beyond complement regulation. Trends Immunol 25: 496–503.
- 495 13. Lukacik P, Roversi P, White J, Esser D, Smith G, et al. (2004) Complement regulation  
496 at the molecular level: the structure of decay-accelerating factor. Proc Natl Acad Sci  
497 USA 101: 1279–1284.

- 498 14. Liszewski MK, Farries TC, Lublin DM, Rooney IA, Atkinson JP (1995) Control of the  
499 complement system. *Adv Immunol* 61: 201–283.
- 500 15. Chauhan A, Moore T (2006) Presence of plasma complement regulatory proteins  
501 clusterin (apo j) and vitronectin (s40) on circulating immune complexes (cic). *Clin  
502 Exp Immunol* 145: 398–406.
- 503 16. Zewde N, Gorham Jr RD, Dorado A, Morikis D (2016) Quantitative modeling of the  
504 alternative pathway of the complement system. *PLoS one* 11: e0152337.
- 505 17. Hirayama H, Yoshii K, Ojima H, Kawai N, Gotoh S, et al. (1996) Linear systems analy-  
506 sis of activating processes of complement system as a defense mechanism. *Biosys-  
507 tems* 39: 173–185.
- 508 18. Korotaevskiy AA, Hanin LG, Khanin MA (2009) Non-linear dynamics of the comple-  
509 ment system activation. *Math Biosci* 222: 127–143.
- 510 19. Liu B, Zhang J, Tan PY, Hsu D, Blom AM, et al. (2011) A computational and experi-  
511 mental study of the regulatory mechanisms of the complement system. *PLoS Comput  
512 Biol* 7: e1001059.
- 513 20. Morad HO, Belete SC, Read T, Shaw AM (2015) Time-course analysis of c3a and  
514 c5a quantifies the coupling between the upper and terminal complement pathways in  
515 vitro. *J Immunol Methods* 427: 13–18.
- 516 21. Morgan BP, Harris CL (2015) Complement, a target for therapy in inflammatory and  
517 degenerative diseases. *NAT REV DRUG DISCOV* 14: 857-877.
- 518 22. Luan D, Zai M, Varner JD (2007) Computationally derived points of fragility of a human  
519 cascade are consistent with current therapeutic strategies. *PLoS Comput Biol* 3:  
520 e142.
- 521 23. Nayak S, Salim S, Luan D, Zai M, Varner JD (2008) A test of highly optimized tol-  
522 erance reveals fragile cell-cycle mechanisms are molecular targets in clinical cancer  
523 trials. *PLoS One* 3: e2016.

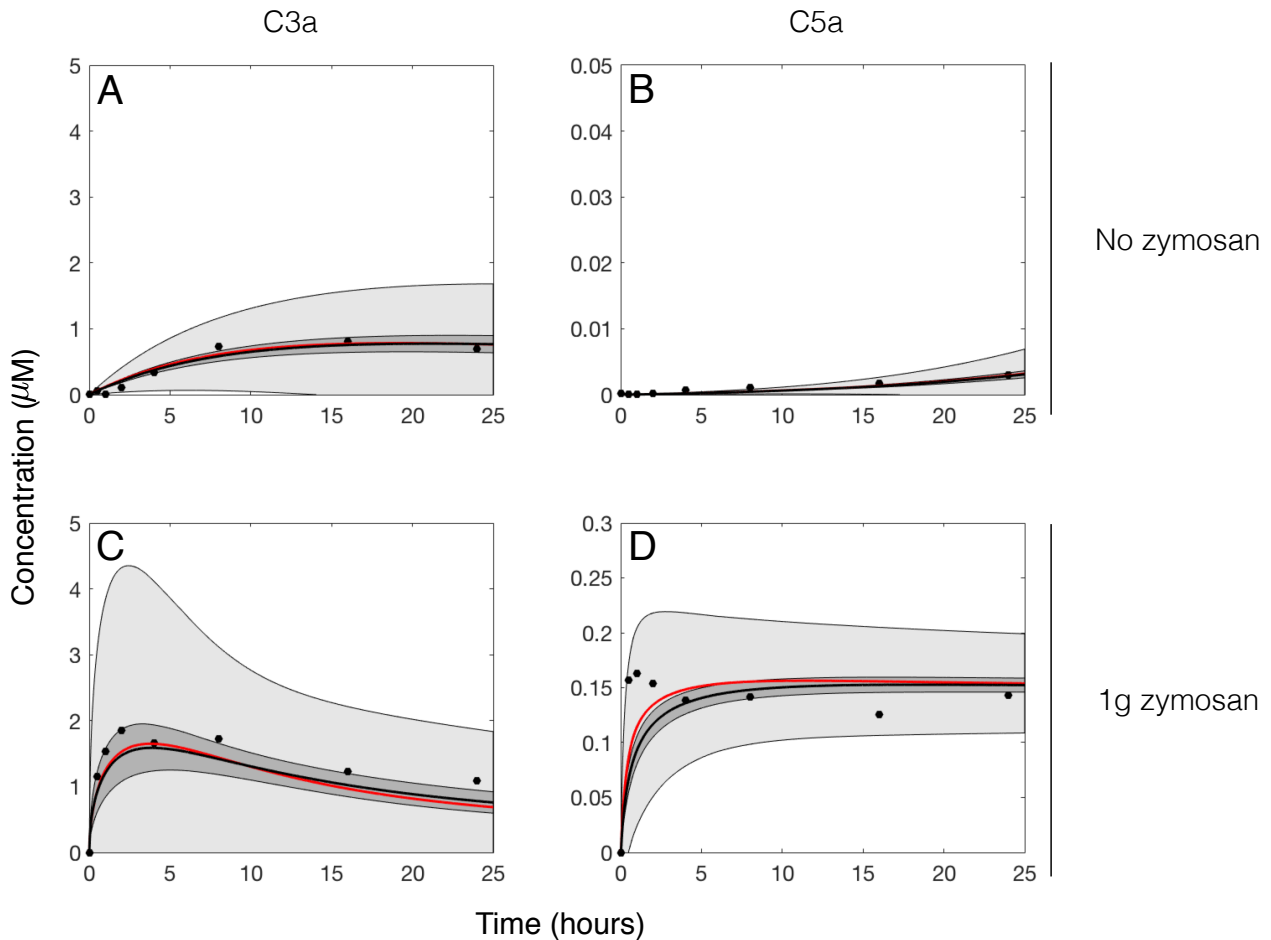
- 524 24. Tasseff R, Nayak S, Salim S, Kaushik P, Rizvi N, et al. (2010) Analysis of the molecular  
525 networks in androgen dependent and independent prostate cancer revealed fragile  
526 and robust subsystems. PLoS One 5: e8864.
- 527 25. Rice NT, Szlam F, Varner JD, Bernstein PS, Szlam AD, et al. (2016) Differential con-  
528 tributions of intrinsic and extrinsic pathways to thrombin generation in adult, maternal  
529 and cord plasma samples. PLoS One 11: e0154127.
- 530 26. Héja D, Harmat V, Fodor K, Wilmanns M, Dobó J, et al. (2012) Monospecific inhibitors  
531 show that both mannan-binding lectin-associated serine protease-1 (masp-1) and-2  
532 are essential for lectin pathway activation and reveal structural plasticity of masp-2. J  
533 Biol Chem : 20290–20300.
- 534 27. Roguska M, Splawski I, Diefenbach-Streiber B, Dolan E, Etemad-Gilbertson B, et al.  
535 (2014) Generation and characterization of Ifg316, a fully-human anti-c5 antibody for  
536 the treatment of age-related macular degeneration. Investigative Ophthalmology &  
537 Visual Science : 3433–3433.
- 538 28. Melis JP, Strumane K, Ruuls SR, Beurskens FJ, Schuurman J, et al. (2015) Com-  
539 plement in therapy and disease: Regulating the complement system with antibody-  
540 based therapeutics. Molecular immunology : 117–130.
- 541 29. Weston-Davies WH, Nunn MA, Pinto FO, Mackie IJ, Richards SJ, et al. (2014) Clin-  
542 ical and immunological characterisation of coversin, a novel small protein inhibitor of  
543 complement c5 with potential as a therapeutic agent in pnh and other complement  
544 mediated disorders. Blood : 4280–4280.
- 545 30. Epstein D, Kurz JC (2007). Complement binding aptamers and anti-c5 agents useful  
546 in the treatment of ocular disorders. US Patent App. 12/224,708.
- 547 31. Borodovsky A, Yucius K, Sprague A, Banda NK, Holers VM, et al. (2014) Aln-cc5, an  
548 investigational rnai therapeutic targeting c5 for complement inhibition. Complement  
549 20: 40.

- 550 32. Sissons J, Liebowitch J, Amos N, Peters D (1977) Metabolism of the fifth component  
551 of complement, and its relation to metabolism of the third component, in patients with  
552 complement activation. *J Clin Invest* 59: 704.
- 553 33. Swaak A, Hannema A, Vogelaar C, Boom F, van Es L, et al. (1982) Determination of  
554 the half-life of c3 in patients and its relation to the presence of c3-breakdown products  
555 and/or circulating immune complexes. *Rheumatol Int* : 161–166.
- 556 34. Noris M, Galbusera M, Gastoldi S, Macor P, Banterla F, et al. (2014) Dynamics of  
557 complement activation in ahus and how to monitor eculizumab therapy. *Blood* : 1715–  
558 1726.
- 559 35. Schwaeble HW, Stover CM, Tedford CE, Parent JB, Fujita T (2011). Methods for  
560 treating conditions associated with masp-2 dependent complement activation. US  
561 Patent 7,919,094.
- 562 36. Katschke KJ, Wu P, Ganesan R, Kelley RF, Mathieu MA, et al. (2012) Inhibiting al-  
563 ternative pathway complement activation by targeting the factor d exosite. *Journal of*  
564 *Biological Chemistry* : 12886–12892.
- 565 37. Hu X, Holers VM, Thurman JM, Schoeb TR, Ramos TN, et al. (2013) Therapeutic in-  
566 hibition of the alternative complement pathway attenuates chronic eae. *Mol Immunol*  
567 : 302–308.
- 568 38. Bansal R (2014). Humanized and chimeric anti-properdin antibodies. US Patent  
569 8,664,362.
- 570 39. Vogel CW, Fritzinger DC, Hew BE, Thorne M, Bammert H (2004) Recombinant cobra  
571 venom factor. *Molecular immunology* : 191–199.
- 572 40. Sagar A, Varner JD (2015) Dynamic modeling of the human coagulation cascade  
573 using reduced order effective kinetic models. *Processes* 3: 178.
- 574 41. Sobol I (2001) Global sensitivity indices for nonlinear mathematical models and their  
575 monte carlo estimates. *MATH COMPUT SIMULAT* 55: 271 - 280.

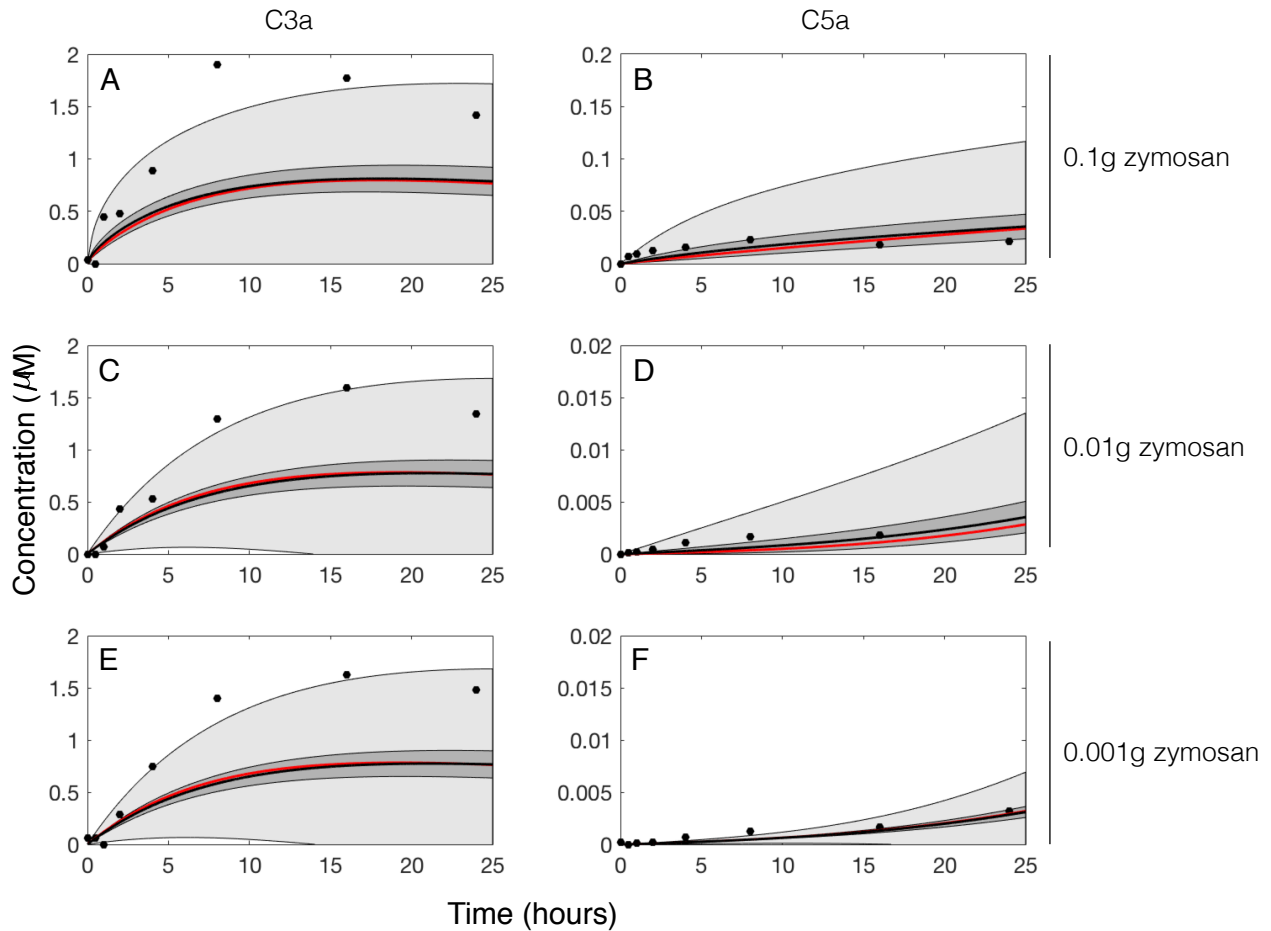
- 576 42. Saltelli A, Annoni P, Azzini I, Campolongo F, Ratto M, et al. (2010) Variance based  
577 sensitivity analysis of model output. design and estimator for the total sensitivity index.  
578 Comput Phys Commun 181: 259–270.
- 579 43. Herman J. Salib: Sensitivity analysis library in python (numpy). con-  
580 tains sobol, morris, fractional factorial and fast methods. available online:  
581 <https://github.com/jdherman/salib>.
- 582 44. Tasseff R, Nayak S, Song SO, Yen A, Varner JD (2011) Modeling and analysis  
583 of retinoic acid induced differentiation of uncommitted precursor cells. Integr Biol  
584 (Camb) 3: 578-91.



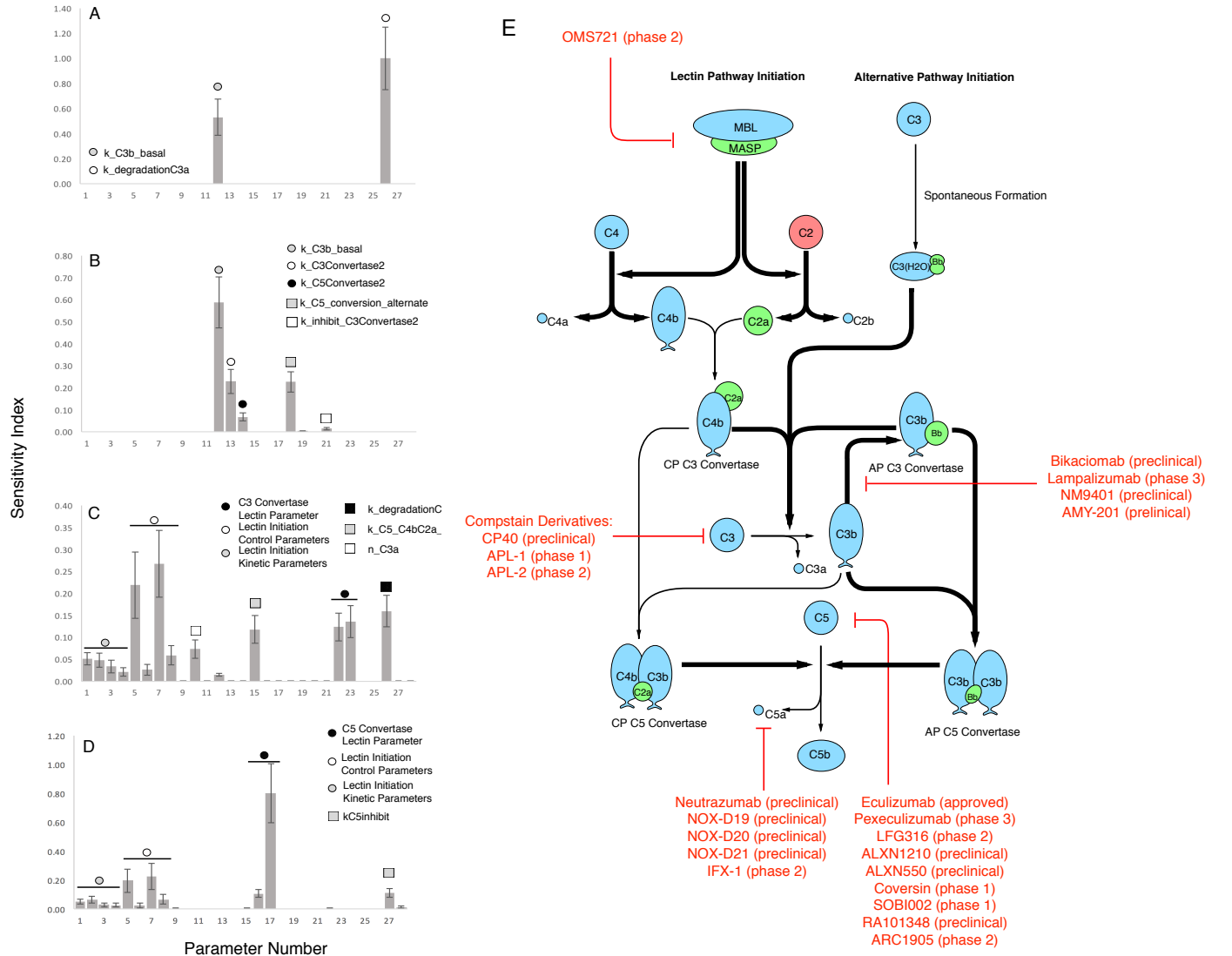
**Fig. 1:** Simplified schematic of the human complement system. The complement cascade is activated through three pathways: the classical, the lectin, and the alternate pathways. Complement initiation results in the formation of classical or alternative C3 convertases, which amplify the initial complement response and signal to the adaptive immune system by cleaving C3 into C3a and C3b. C3 convertases further react to form C5 convertases which catalyze the cleavage of the C5 complement protein to C5a and C5b. C5b is critical to the formation of the membrane attack complex (MAC), while C5a recruits an adaptive immune response.



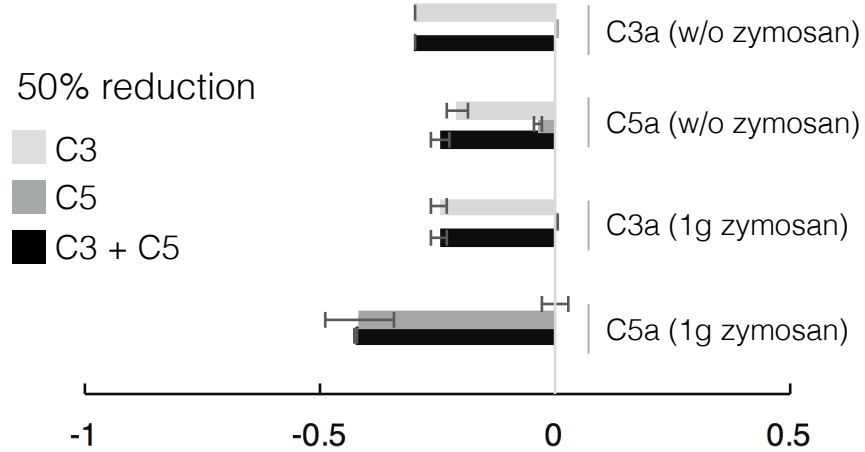
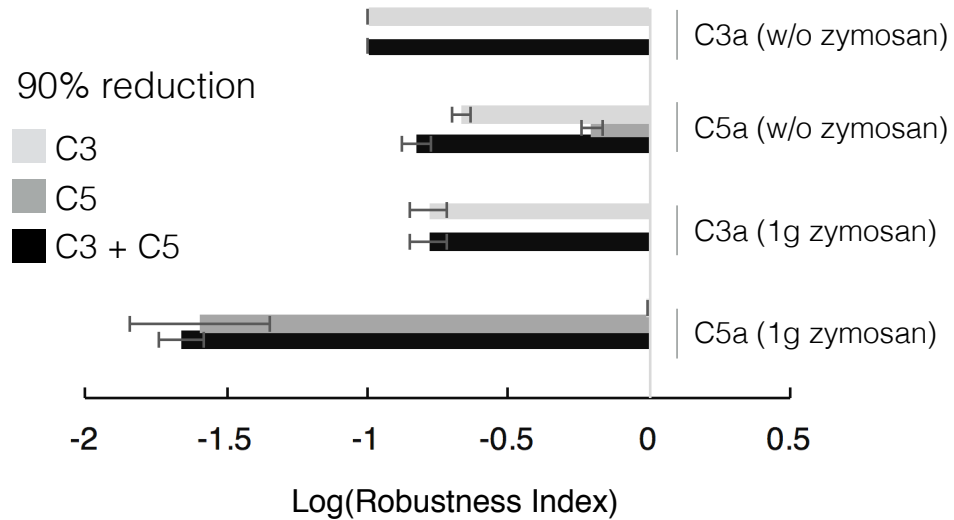
**Fig. 2:** Reduced order complement model training. Model parameters were estimated using Dynamic Optimization with Particle Swarms (DOPS) from C3a and C5a measurements with and without zymosan (20). The model was trained using C3a and C5a data generated from the alternative pathway (**A–B**) and lectin pathway initiated with 1g zymosan (**C–D**). The solid red line shows the simulation with the best-fit parameter set, the solid black lines show the simulated mean value of C3a or C5a for the ensemble ( $N = 50$ ). The dark shaded region denotes the 99% confidence interval of the simulated mean concentrations, while the light shaded region denotes the 99% confidence interval of the best-fit simulation for C3a and C5a. All initial conditions were assumed to be at their physiological serum levels unless otherwise noted.



**Fig. 3:** Reduced order complement model predictions. The reduced order coagulation model parameter estimates were tested against data not used during model training (20). Simulations of C3a and C5a generated in the lectin pathway using 0.1g, 0.01g, and 0.001g zymosan were compared with the corresponding experimental measurement. The solid red line shows the simulation with the best-fit parameter set, the solid black lines show the simulated mean value of C3a or C5a for the ensemble ( $N = 50$ ). The dark shaded region denotes the 99% confidence interval of the simulated mean concentrations, while the light shaded region denotes the 99% confidence interval of the best-fit simulation for C3a and C5a. All initial conditions were assumed to be at their physiological serum levels unless otherwise noted.



**Fig. 4:** Global sensitivity analysis of the reduced order complement model. Sensitivity analysis was conducted on the four cases used for model training. **A:** Sensitivity of the C3a residual at w/o zymosan, **B:** Sensitivity of the C5a residual at w/o zymosan, **C:** Sensitivity of the C3a residual at 1g zymosan, and **D:** Sensitivity of the C5a residual at 1g zymosan. The bars denote the mean total sensitivity index for each parameter, while the error bars denote the 95% confidence interval. **E:** Pathways controlled by the sensitivity parameters. Bold black lines indicate the pathway involves one or more sensitive parameters, while the red lines show current therapeutics targets. Current complement therapeutics were taken from the review of Morgan and Harris (21).

**A****B**

**Fig. 5:** Robustness analysis of the complement model with respect to C3 and C5 initial conditions. Robustness analysis was conducted on the four cases used for model training: C3a alternate (w/o zymosan), C5a alternate (w/o zymosan), C3a lectin (1g zymosan), and C5a lectin (1g zymosan), by reducing the initial concentration of C3 and/or C5 by 50% or 90 %. **A:** Robustness results for a 50% decrease in the C3, C5, or C3 and C5 initial condition. **B:** Robustness results for a 90% decrease in the C3, C5, or C3 and C5 initial condition. The bars denote the log-transformed robustness index while error bars denote one standard deviation. At zero, the perturbed initial concentration has no impact on the measured output. A log-transformed robustness index less than zero indicates a negative relation between the perturbed initial concentration and the measured output.